Journal of Information Hiding and Multimedia Signal Processing ©2021 ISSN 2073-4212
Ubiquitous International Volume **12**, Number **2**, June **2021**

Implementation of Chaotic Sequences on UWB Wireless Communication in Presence of NBI

Hany A. A. Mansour

Department of Electronic Warfare
Military Technical College, Kobry ELkobba, Cairo, Egypt
hnhn118799@mtc.edu.eg

Received December 2020; revised February 2021

Abstract. *Recently, chaotic sequences attracted much attention due to its promising features. Chaotic sequences have many privileges over the other tarditional sequences, that encourage the researches to apply them as an alternative sequence in many applications. The Direct Sequence Ultra-Wideband (DS-UWB) is one of these applications, in which the PN codes are replaced with the chaotic sequences to improve and enhance the performance. In this paper, the performance of Impulse Radio (IR) ultra-wideband in presence of Narrow Band Interference (NBI) is analytically investigated. A closed form of the analytical formula is presented under effect of flat fading channel. The NBI is modeled as the Orthogonal Frequency Division Multiplexing (OFDM) based IEEE802.11n standard signal. Statistical comparison and evaluation of the proposed chaotic code sequence are presented, and applied instead of the PN codes. In addition, a new code word design is proposed which has the capability of producing a null at the operating frequency of the in-band NBI signal. Thus, allowing the coexistence between the UWB and in-band high power operating standards. The results show that the proposed scheme can be considered a promising candidate for wireless sensor communication networks.*
Keywords: Chaotic codes; DS-UWB; Wireless sensor networks; Log-normal flat fading channel and narrow band interference.

1. **Introduction.** It is found that chaotic sequences are promising sequences to be applied in various fields due to its attractive properties compared to the other traditional sequences. Chaotic sequences are wide band, non-periodic, however they are non-converging and bounded, founded in non-linear dynamical systems. In addition, chaotic sequences are deterministic, random like, and very difficult to intercept, predict, decode, recover and reconstruct [1, 2]. Chaotic sequences can be generated from chaotic maps based on a certain constrains and specific initial conditions [3]. These conditions give the chaotic sequences its privileges over the other sequences such as the pseudo random noise (PN) sequences. One of these privileges is the flexibility of the code length, which enable the user to generate the sequences with any unconditioned length.

In addition, the number of the generated chaotic sequence doesn't depend on the shift register, it depends on and sensitive to the initial conditions. This sensitivity gives the availability to generate a huge number of sequences according to the available range of the initial condition. This feature becomes very helpful in increasing the system capacity in the applications of Multiple Accesses (MA) [4]. Moreover, it is proven that chaotic sequence is very hard to be recovered, since it depends on both the generated map and the specified initial condition [5]. These attractive features lead to apply the chaotic codes in varies applications such as communications [6], MC-CDMA [7,8], OFDM [9–12],

underwater acoustic communication [13], data encryption [14–16], image encryption [17–20], ultra-Wideband (UWB) communications [21,22], in addition to many other disciplines [23–26] .

The issue of coexistence of UWB with other operating standards and their impact on its performance had been investigated in many previous researches. In [27] a spectrum shaping technique in direct sequence ultra-wideband (DS-UWB) communication systems was proposed. The proposed pulse introduces multiple spectral nulls to limit the interference impact of high power coexisting narrow band signals. In [28, 29] an Orthogonal Complementary Code (OCC)-based UWB system with modified chirp wave forms was proposed to mitigate the impact of multiple interference signals.

In this paper, improved chaotic sequences are presented and applied to UWB communication signals in order to produces nulls at certain predetermined frequencies in Log-normal flat fading channels. These frequencies are the operating frequencies of high power in-band interference standards. The proposed scheme can be used as an application for wireless communication sensor networks. The main contribution of this paper is to present a statistical analysis of different chaotic codes to produce improved sequences with enhanced features for different code lengths. in addition, investigate the Bit Error Rate (BER) performance of IR chaotic UWB communication system in presence of NBI model as the OFDM-based IEEE802.11n communication standard in Log-normal flat fading channel. Moreover, A closed form analytical formula is derived to represent the BER performance of the chaotic UWB communication system in presence of NBI standard signal. Finally, design a code word sequence that is capable to produce multiple nulls at the high power in-band NBI operating frequencies to mitigate its impact.

The paper is organized as follows. In section 2 the signal models for UWB, the narrow band interference (NBI) operating standard and their associated channel models are presented. Section 3 illustrates the performance analysis of the UWB communication system in presence of NBI standard signal. The statistical analyses of different chaotic codes with different code lengths are discussed in section 4. In section 5 the idea of designing the proposed improved chaotic code sequence is presented analytically. Analytical and simulation results are presented in section 6. Finally, section 7 draws the conclusions.

2. **System Model.** The considered UWB transmitted signal is the IR Direct Sequence Binary Phase Shift Keying (DS-BPSK) UWB communication signal. It can be represented as

$$S^{DS}_{BPSK}(t) = \sqrt{E_b} \sum_i d_i \sum_{j=-\infty}^{\infty} C_j \, p(t - j\,T_f \, - iT_b) \tag{1}$$

Where $p(t)$ is transmitted pulse shape, d_i is the ith transmitted equally likely binary data bits, the bit duration $T_b = N_s T_f$ with bit energy E_b. N_s is the number of pulses transmitted per bit and T_f is the frame duration. C_j is the DS bipolar code sequence, $C_j \in -1, +1$.

In this paper, the OFDM based IEEE802.11n standard is considered as the potential interference threat to the performance of the IR-UWB communication systems. According to [30], this OFDM based interference can be considered as the sum of M tones. Then, the NBI signal can be written as

$$I(t) = \sum_{m=1}^{M_i} \sqrt{\frac{2I}{M_i}} \cos(2\pi \, f_m \, t + \phi_m) \tag{2}$$

Where f_m is the mth tone interference frequency, ϕ_m is the independent and identically distributed random phases, and I is the total transmitted power of the interference signal.

It was stated in [31] that although the UWB communication channel is always considered a frequency selective type, yet in some scenarios it can be considered as a flat fading channel. This is due to the fact that in some applications such as the wireless sensor networks, they encounter size and power problem constraints. These constraints impose on each node to simplify its own circuitry. One of the proposed solutions was the use of a single finger RAKE receiver as a sub-optimal solution to this problem. In this case, one can model the UWB communication channel as a flat fading type.

The received signal can be written as

$$r(t) = S_r(t) + I_r(t) + Z(t) \tag{3}$$

Where $Z(t)$ is the Additive White Gaussian Noise (AWGN) and $S_r(t)$ is the received desired UWB communication signal which can be written as

$$S_r^{DS-BPSK}(t) = \sqrt{E_b} \sum_i d_i \sum_{j=-\infty}^{\infty} a_s \, C_j \, p(t - j\,T_f \, - iT_b \, - \tau_s) \tag{4}$$

And $I_r(t)$ is the received interference signal which can be written as

$$I_r(t) = \sqrt{\frac{2I}{M_i}} \sum_{m=1}^{M_i} \alpha_i \cos(2\pi \, f_m \, t + \phi_m) \tag{5}$$

Where α_i is the ith Rayleigh distributed channel gain and τ_i is the ith corresponding time delay for the M_i tones.

3. **Performance Analysis in Presence of NBI.** Following the results presented in [24], the BER performance of the IR-UWB wireless sensor communication devises in flat fading channel can be written as

$$P_e = \frac{1}{\sqrt{\pi}} \sum_{i=1}^{N} \beta_i [Q(\sqrt{\chi \exp(2\sqrt{2} q_i \, \sigma_r \, + 2\mu_r)})] \tag{6}$$

where β_i and q_i represent the Hermite polynomial weights and roots respectively. N are the number of samples points used for this approximation. μ_r and σ_r are the mean and standard variation of the Log-normal random variable. Finally, χ is the signal to interference plus noise power ratio, which can be written as

$$\chi = [(\frac{2E_b}{N_o})^{-1} + (\frac{4SIR.M_i.T_b}{\sum_n^{N_i} |H(f_n)|^2})^{-1}]^{-1} \tag{7}$$

where SIR is the signal to interference power ratio and $H(f)$ is the transfer function of the matched filter receiver. The first term represents the impact of the AWGN, while the second term represents the impact of interference.

The transfer function of the matched filter receiver can be modeled as for DS-BPSK case

$$H^{DS-BPSK}(f) = 2|P(f)|| \sum_{k=0}^{N_s-1} C_k \exp{(j2\pi f k T_f)}| \tag{8}$$

where $P(f)$ is the Fourier transform of the UWB pulse, which in our work is considered a six derivative Gaussian pulse to match the UWB spectral emission mask defined by FCC. It can be written as

$$P(f) = \frac{8\pi^3}{3\sqrt{1155 N_s}} \tau_p^{\frac{13}{2}} f^6 \exp{(-\frac{\pi f^2 \tau_p^2}{2})} \tag{9}$$

It can be noted form equation 6 to equation 9 that the IR-DS-BPSK UWB BER performance depends on PN sequence. Thus, with the suitable selection of this sequence, it

can be expected to generate a null in the frequency spectrum exactly at the operating frequency of the NBI OFDM based IEEE802.11n standard. This can reduce the effect of the NBI on the BER performance of the DS-BPSK UWB wireless sensor devises and allow the coexistence of other standards operating in the same frequency band. It is stated in [18] that the PSD of the DS-BPSK UWB signal can be represented as

$$P_{DS}(F) = \frac{|P(f)|^2}{T_f} \sum_{m=-\infty}^{\infty} R_d(m).e^{-j2\pi f_m T_f} = \frac{|P(f)|^2}{T_f}.P_c(f) \tag{10}$$

Where R_d (m) is the even function autocorrelation of the d_i data bits, $P(f)$ is the pulse shaping function, and $P_c(f)$ is the pseudo random code spectrum function.

$$P_c(F) = \sum_{m=-\infty}^{\infty} R_d(m).e^{-j2\pi f_m T_f} \tag{11}$$

4. **Chaotic Map Generation.** in this section, the presented sequence is generated and modified to improve and enhance its properties and features [32]. The presented sequences are the Zero-Mean (ZM) sequence based on the logistic maps. The basic real value chaotic sequence of the basic logistic map can be represented as

$$x_{i+1} = Rx_i(1 - x_i), \qquad x_i \in (0, 1) \tag{12}$$

Where, x_{i+1} is the new value generated from the old value x_i, R is the bifurcation parameter. In order to generate the basic binary chaotic sequence in this stage, the real values of the basic chaotic sequence are mapped to the binary values according to the rule:

$$X_1 = (-1)^{round(g[x(t)])} \tag{13}$$

Where $g(x(t))$ representing the general applied map function used to generate the chaotic sequence. Actually, there are various methods can be used to map the real values of the chaotic code into the binary values such as the digitization method, the threshold method, and the zero mean threshold method [9]. The first method is applied to obtain the traditional sequence, and the third method is applied to generate the ZM sequence as

$$x_1 = sign(g(x(t) - mean[x(t)])) \tag{14}$$

This method depends on shifting the real value for the basic chaotic code by its mean value and generates a new basic sequence $g(x)$ which has a zero mean. The binary values will then obtained by taking the sign function of the new zero mean sequence $g(x)$.

The orthogonal codes are found by comparing the generated output codes with all the available orthogonal sequences to the reference signal. The different generated codes are generated by changing the bifurcation parameter through range from 0.1 to 4 with step of 0.1, and changing the range of the initial condition from 0.01 to 0.99 with step 0.01.

Table 1 discusses the balance property, which is defined as the ratio between the number of zeros (or ones) to the total code length. In this paper, the applied results are the ratio of the ones to the total code length. The table shows the balance value for the raw logistic code, ZM, Self Balance (SB), Zero Mean Self Balance (ZMSB), and compared with the Gold code as traditional PN sequence. The analysis is performed for different code length starting from 16 up to 512. From the table, it can be noted that, (I) the SB, and ZMSB have perfect balance equal to 0.5. (II) The raw logistic code has generally the worst balance compared with all the other codes, since there is not any enhancement performed. (III) The attitude of the Gold code is less than the ZM code regarding to the short length, and improved as the code length increased. Table 2 represents the analysis of the normalized maximum autocorrelation side lobe (NMACSL) property. The ideal case of the autocorrelation of any spreading code is to obtain the δ-like autocorrelation

Table 1. Balance Property

Code Type / Code Length	16	32	64	128	256	512
Raw Logistic	0.46875	0.53125	0.52344	0.52734	0.52539	0.54785
ZM Logistic	0.5	0.48438	0.47656	0.48047	0.48438	0.47949
SB Logistic	0.5	0.5	0.5	0.5	0.5	0.5
ZMSB Logistic	0.5	0.5	0.5	0.5	0.5	0.5
Gold Sequences	0.5333	0.45161	0.44444	0.47244	0.50196	0.48532

Table 2. Normalized Maximum Auto correlation Side Lobe

Code Type / Code Length	16	32	64	128	256	512
Raw Logistic	0.25	0.125	0.125	0.10938	0.11719	0.0664
ZM Logistic	0.25	0.125	0.125	0.10938	0.125	0.0625
SB Logistic	0.375	0.3125	0.125	0.09375	0.09375	0.085938
ZMSB Logistic	0.25	0.3125	0.125	0.125	0.09375	0.082031
Gold Sequences	0.0333	0.14516	0.11905	0.066929	0.060784	0.03229

Table 3. Cross Correlation Property

Code Type / Code Length	16	32	64	128	256	512
Raw Logistic	0.085938	0.072266	0.048828	0.037598	0.025024	0.017845
ZM Logistic	0.0625	0.080078	0.048828	0.037476	0.025238	0.017937
SB Logistic	0.03125	0.039063	0.049805	0.035156	0.027954	0.019211
ZMSB Logistic	0.125	0.039063	0.04687	0.033936	0.02771	0.018906
Gold Sequences	0.094444	0.078335	0.065903	0.041155	0.030861	0.027274

function, i.e.$C_a(\tau) = \sum_{i=1}^{N} x_i x_{i+\tau} = \delta(\tau)$, where N is the code length. However, in the real case this condition is not achieved, and many side lobes are generated. It is desired for the autocorrelation function to be near as much as possible to the δ-like, which mean minimizing the side lobes compared to the main lobe. Regarding to table 2, it is clear that (i) for the short lengths, the NMACSL values of the all the chaotic codes are large compared to the Gold code, which indicate that the autocorrelation function of the Gold code is significantly better than that of the chaotic sequences. (ii) As the code length increased, the NMACSL values of the chaotic codes are improved and become comparable with that Gold code. (iii) Regarding to the chaotic codes, it is noted that the SB, and ZMSB has the worst attitude compared to the raw logistic and ZM. This note gives an indication that the SB operation has negative effect on the NMACSL property.

Table 3 discusses the different cross correlation values for the different proposed chaotic codes, in addition the gold code. The obtained results can be concluded as (i) generally, the chaotic sequences have better cross correlation values over the Gold code. This feature leads to enhance the performance of the chaotic codes over the Gold code especially in the dense environment of the multiple access interference. (ii) As a general trend, the cross correlation values are improved as the code length increased. (iii) Regarding to the chaotic codes, it is noted that nearly all the chaotic sequences have the same attitude all over the code length.

5. **Code-Word Design.** The main objective in this section is to design a code-word C, which is capable to generate a null at a specific frequency, f_i. This predetermined frequency will be the same operating frequency of the NBI signal. It can be noted that

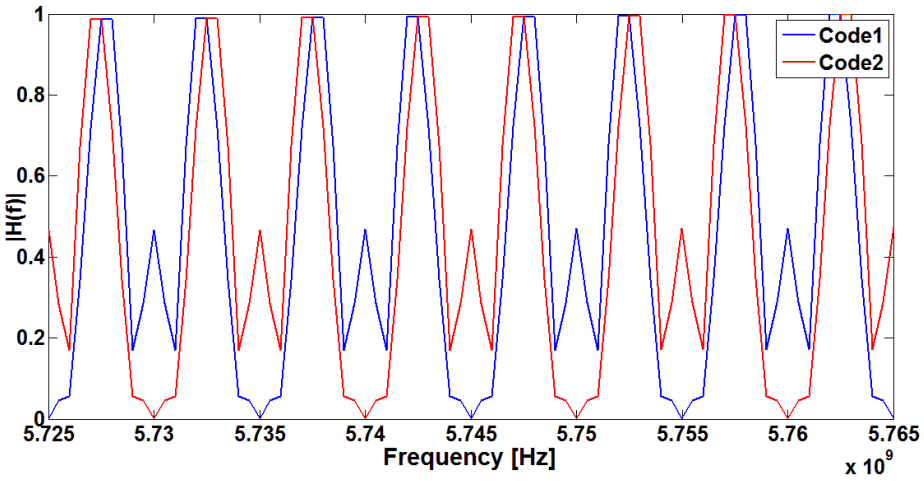

FIGURE 1. Two code-words with different code design function.

.

from equation 10 that the PSD of the DS-UWB signal consists of two parts. The first one depends on the used pulse shape, which is considered as the six derivative Gaussian pulse. The second part, which is the most important, is depending on the code-word C. The code-word in the frequency domain can be written as

$$C(f) = |\sum_{k=0}^{N_s-1} C_k . \exp(j2\pi f_k T_f)| \tag{15}$$

It can be seen that it depends on the operating frequency f, code-word C and the frame duration T_f. A null can be generated at a specific frequency by solving the generated equation which will be function of the code-word. For example, assuming $N_s = 6$, $T_f = 100N_s$, $\tau_p = 0.2N_s$, $f = 5.745GHz$. The generated equation in this case will be

$$C(f) = C_1 - C_2 + C_3 - C_4 + C_5 - C_6 \tag{16}$$

Any combination of the code-word that fulfills such equation will produce a null at the predetermined frequency. Figure 1 depicts such idea with using two code-words. The first one is [-1 -1 1 1 -1 -1] which fulfills the equation, whereas the second code-word doesn't which is [-1 1 1 -1 -1 1]. It can be seen that the first code-word produces a null at the predetermined frequency while the other code-word doesn't.

6. **Numerical and Simulation Results.** In this section, the Chaotic-BPSK UWB wireless sensor communication system is considered. The following parameters are chosen: a six derivative Gaussian received pulse with a pulse duration $\tau_p = 0.1N_s$, a frame length $T_f = 30N_s$. The two possible spreading sequences: $[C_1]$ = [-1, -1, +1, -1, -1, +1, -1, -1, -1, -1, +1, -1, -1, +1, +1, -1, -1, +1, +1, -1] and $[C_2]$ = [+1, +1, -1, -1, - 1, +1, +1, -1, -1, +1, -1, +1, +1, -1, +1, -1, -1, +1, +1, -1] of length $N_s = 20$. The IEEE802.11n NBI standard signal is assumed to be operated at $5.2GHz$. The frequency domain representation of the normalized matched filter transfer function for two mentioned chaotic code sequences is presented in Figure 2. This normalized matched filter transfer functions are presented in the same operating frequency range of the standard IEEE802.11n NBI signal at $5.2GHz$. It can be seen that the normalized matched filter transfer function of the second chaotic code sequence produces a null at exactly $5.2GHz$, whereas the normalized matched filter transfer function of the first chaotic code sequence fails to do so. Figure 3 depicts the PSD of the proposed chaotic BPSK UWB wireless sensor communication signal. It can

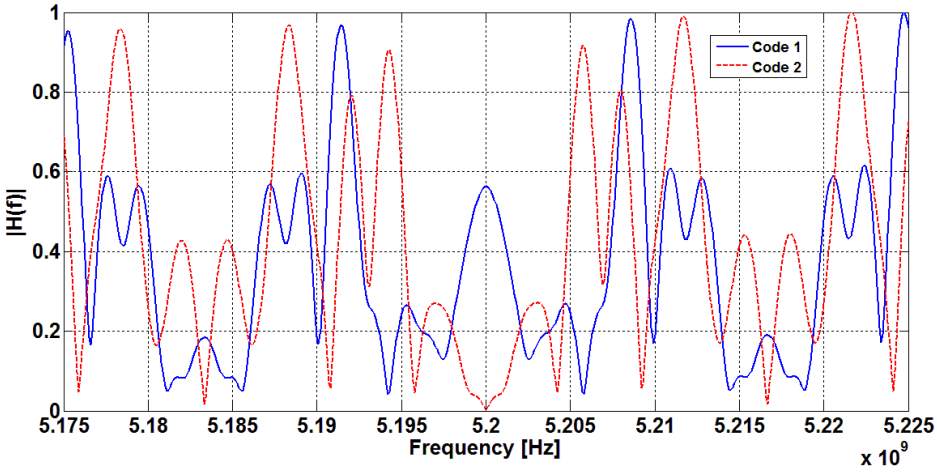

FIGURE 2. Two different chaotic code normalized transfer functions of the matched filter receiver at frequency range around 5.2GHz.

.

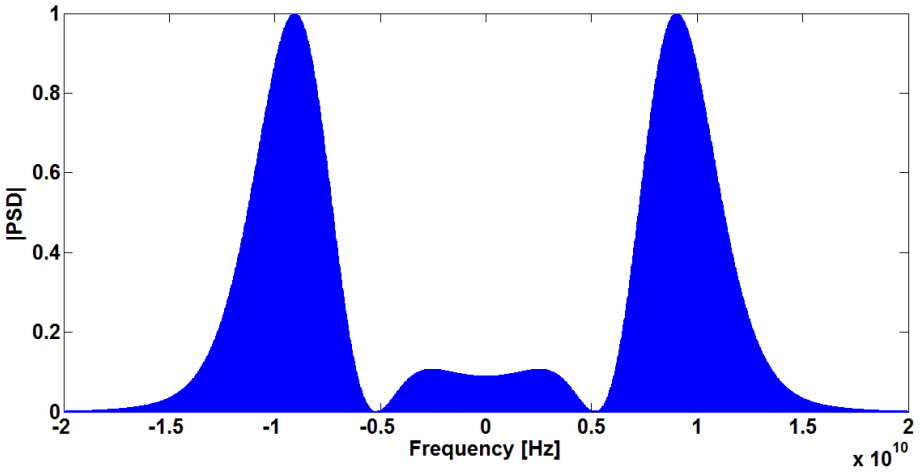

FIGURE 3. Normalized PSD for the chaotic BPSK UWB wireless sensor communication signal.

.

be seen that a null is produced at exactly $5.2GHz$ which is the operating frequency of the IEEE802.11n standard NBI signal. Figure 4 and Figure 5 represent a BER performance comparison of the BPSK UWB wireless sensor communication signals using two possible chaotic code sequences. This comparison is presented in absence/presence of the OFDM based IEEE802.11n standard NBI signal in log-normal flat fading channel with dB-spread value $= 2dB$. The IEEE802.11n NBI signal is operated at $5.2GHz$. These two figures are achieved at $SIR = -10$ dB and -20 dB respectively. It can be seen that the usage of the second chaotic code sequence which produces a null at 5.2GHz outperforms the first chaotic code sequence. It can also be noted that there was a performance degradation equals to $2dB$ at $BER = 10^{-3}$ with the usage of the second chaotic code sequence in presence of IEEE802.11n NBI with respect to the scenario of absence of the NBI signal at $SIR = -20$ dB. Whereas, in the scenario of $SIR = -10$ dB there was a performance degradation equals to $1dB$ at $BER = 10^{-5}$ with the usage of the second chaotic code

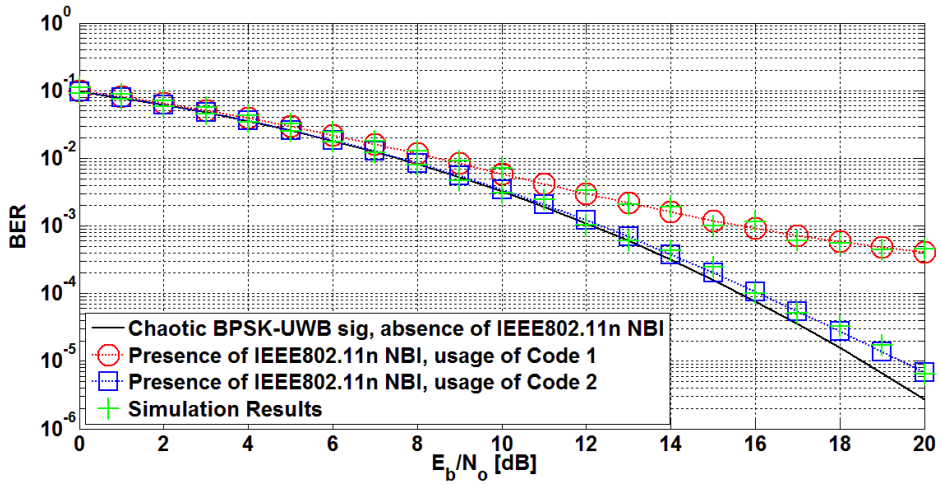

FIGURE 4. BER performance for BPSK UWB wireless sensor communication signal using two chaotic code sequences in presence of IEEE802.11n NBI, SIR = -10dB, in Log-normal Flat fading channel.

.

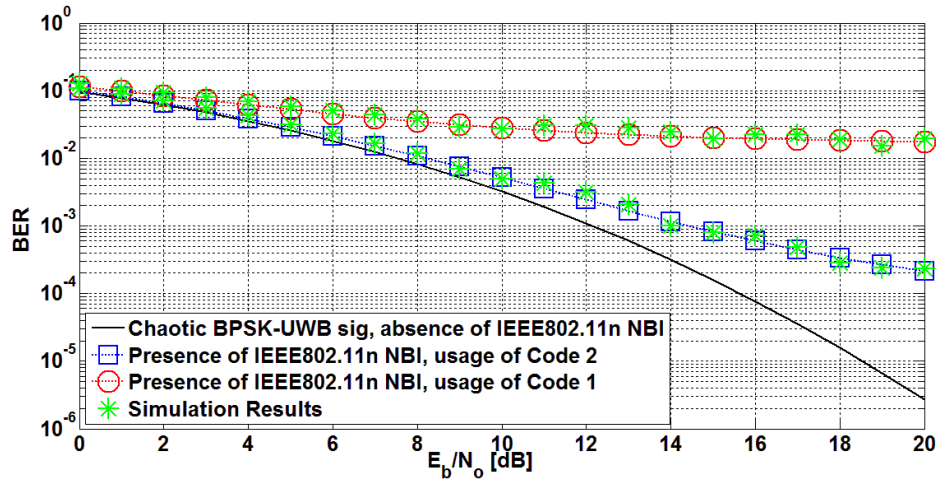

FIGURE 5. BER performance for BPSK UWB wireless sensor communication signal using two chaotic code sequences in presence of IEEE802.11n NBI, SIR = -20dB, in Log-normal Flat fading channel.

.

sequence in presence of IEEE802.11n NBI with respect to the scenario of absence of the NBI signal.

Also, it can be seen that the performance of the UWB communication system is severely deteriorated in presence of NBI signal with the usage of the first code. The simulation results are in a good match with the derived analytical ones.

7. **Conclusion.** In this work, the performance of the chaotic code UWB communication system was investigated in presence of high power in band WIFI IEEE802.11n standard interference signal. The considered channel was the Log-normal flat fading channel to provide the simplicity, low power and low cost requirements for wireless communication sensor nodes. A closed form expression was analytically evaluated for the BER performance of the chaotic UWB communication system in presence of NBI signal. It was

presented that the performance of the UWB was severely deteriorated in presence of high power NBI signal.

Statistical analyses were presented to improve the chosen chaotic code sequence properties along with an analytical code-word design procedure was presented. The proposed code-word has the capability to produce multiple nulls in the UWB operating spectrum. These nulls are predetermined and set exactly at the operating frequencies of the NBI signals. The proposed scheme proved the ability to mitigate the impact of NBI signal analytically and validated with the simulation results.

REFERENCES

[1] K. Kashyap and T. Sharma, "Dynamic Logistic Map-Based Spread Spectrum Modulation in Wireless Channels",International Journal of Applied Evolutionary Computation, vol. 9, no. 2, pp. 52-65, 2018. Available:10.4018/ijaec.2018040105

[2] H. Bao, Z. Hua, N. Wang, L. Zhu, M. Chen and B. Bao, "Initials-Boosted Coexisting Chaos in a 2-D Sine Map and Its Hardware Implementation," in IEEE Transactions on Industrial Informatics, vol. 17, no. 2, pp. 1132-1140, Feb. 2021, doi: 10.1109/TII.2020.2992438.

[3] S. Liu, "Research on the design and implementation of two dimensional hyper chaotic sequence cipher algorithm," 2017 Sixth International Conference on Future Generation Communication Technologies (FGCT), Dublin, 2017, pp. 1-4, doi: 10.1109/FGCT.2017.8103730.

[4] Anamika Sarma, Kandarpa Kumar Sarma and Nikos Mastorakis, "Orthogonal Chaotic Sequence for Use in Wireless Channels," International Journal of Computers and Communications Vol. 9, 2015.

[5] Hany A. A. Mansour, Ahmed Khamis, Dawid Zydek , Henry Selvaraj, "Performance Analysis and Evaluation of Multi-User Coded Hybrid Spread Spectrum System using Improved Chaotic Sequences," 26th International Conference on System Engineering, 2018.

[6] Chenglong Zhou, "Turbo Trellis-Coded Differential Chaotic Modulation," IEEE Transactions on Circuits and Systems—II: Express Briefs, Vol. 65, No. 2, February 2018.

[7] Jianxin Wang, "Analysis Performance of MC-CDMA Communication System Based on Improved Chebyshev Sequence," 2nd IEEE International Conference on Computer and Communications, 2016

[8] Anna Litvinenko, Arturs Aboltins, "Use of Cross-Correlation Minimization for Performance Enhancement of Chaotic Spreading Sequence Based Asynchronous DS-CDMA System," IEEE Trans, 2016.

[9] Asma Ahmadinejad, Siamak Talebi "Performance evaluation of chaotic spreading sequences in a multi-user MIMO-OFDM system", physical communication 19 (2016) 11-17.

[10] Shuying Li, Yaqin Zhao, and Zhilu Wu, "Design and Analysis of an OFDM-based Differential Chaos Shift Keying Communication System", Journal of Communications Vol. 10, No. 3, March 2015.

[11] F. S. Hasan and A. A. Valenzuela, "Design and Analysis of an OFDM-Based Orthogonal Chaotic Vector Shift Keying Communication System," in IEEE Access, vol. 6, pp. 46322-46333, 2018, doi: 10.1109/ACCESS.2018.2862862.

[12] X. Lu, Y. Shi, W. Li and J. Lei, "Encrypted subblock design aided OFDM with all index modulation," in IET Communications, vol. 14, no. 17, pp. 2924-2930, 27 10 2020, doi: 10.1049/iet-com.2019.0678.

[13] Hany A. A. Mansour, "Analytical and Performance Evaluation of Chaotic Sequences under Effect of Gaussian Mixture Noise," 2019 International Conference on Image, Video and Signal Processing (IVSP 2019), Shanghai, China.

[14] M. Kushnir, A. Semenko, G. Kosovan, N. Bokla and Y. Shestopal, "Increasing the Cryptosecurity of Telecommunication Systems With Spread Spectrum by Using Pseudorandom Sequences Based on Two Ergodic Chaotic Signals," 2019 3rd International Conference on Advanced Information and Communications Technologies (AICT), Lviv, Ukraine, 2019, pp. 455-458, doi: 10.1109/AIACT.2019.8847913.

[15] C. Zhu, S. Li and Q. Lu, "Pseudo-random Number Sequence Generator Based on Chaotic Logistic-Tent System," 2019 IEEE 2nd International Conference on Automation, Electronics and Electrical Engineering (AUTEEE), Shenyang, China, 2019, pp. 547-551, doi: 10.1109/AUTEEE48671.2019.9033389.

[16] I. E. Hanouti, H. E. Fadili, W. Souhail and F. Masood, "A Lightweight Pseudo-Random Number Generator Based on a Robust Chaotic Map," 2020 Fourth International Conference On Intelligent Computing in Data Sciences (ICDS), Fez, Morocco, 2020, pp. 1-6, doi: 10.1109/ICDS50568.2020.9268715.

[17] Y. Luo, X. Ouyang, J. Liu and L. Cao, "An Image Encryption Method Based on Elliptic Curve Elgamal Encryption and Chaotic Systems," in IEEE Access, vol. 7, pp. 38507-38522, 2019, doi: 10.1109/ACCESS.2019.2906052.

[18] S. N. Prajwalasimha, S. R. Kavya and C. Navyakanth, "Digital Image Encryption based on Transformation and Henon Chaotic Substitution," 2019 4th International Conference on Recent Trends on Electronics, Information, Communication & Technology (RTEICT), Bangalore, India, 2019, pp. 1237-1241, doi: 10.1109/RTEICT46194.2019.9016709.

[19] S. Ma, Y. Zhang, Z. Yang, J. Hu and X. Lei, "A New Plaintext-Related Image Encryption Scheme Based on Chaotic Sequence," in IEEE Access, vol. 7, pp. 30344-30360, 2019, doi: 10.1109/ACCESS.2019.2901302.

[20] X. Wang and S. Chen, "Chaotic Image Encryption Algorithm Based on Dynamic Spiral Scrambling Transform and Deoxyribonucleic Acid Encoding Operation," in IEEE Access, vol. 8, pp. 160897-160914, 2020, doi: 10.1109/ACCESS.2020.3020835.

[21] S. K. Shanmugam et al., "Efficient Chaotic Spreading Codes for DS-UWB Communication System," International Conference on Acoustics Speech and Signal Processing, 2016.

[22] Hang Ma, P. Acco, M. Boucheret and D. Fournier-Prunaret, "Chaos-based TOA estimator for DS-UWB ranging systems in multiuser environment," 21st European Signal Processing Conference (EUSIPCO 2013), Marrakech, 2013, pp. 1-5.

[23] Juan Wang, Bo-Wen Pan, Qian-Rui Wang and Qun Ding, "A Chaotic Key Expansion Algorithm Based on Genetic Algorithm", Journal of Information Hiding and Multimedia Signal Processing, Vol. 10, No. 2, pp. 289-299, March 2019

[24] Kai Feng, Xin Huang, Shu-Chuan Chu, John F Roddick and Qun Ding, "An Implementation of Chaotic Pseudo-Random Sequence Generator Based on Pipelined Architecture", Journal of Network Intelligence, Vol. 4, No. 2, pp. 71-79, May 2019

[25] Wangshu Li, Wenhao Yan, Qun Ding, Ruoxun Zhang and Yeh-Cheng Chen, "Discrete Synchronization Method for Continuous Chaotic Systems and Its Application in Secure Communication", Journal of Network Intelligence, Vol. 5, No. 2, pp. 62-76, May 2020

[26] Xintong Wang and Hongfeng Zhu, "A Novel Two-party Key Agreement Protocol with the Environment of Wearable Device using Chaotic Maps," Data Science and Pattern Recognition, Vol. 3(2), pp. 12–23, 2019

[27] Ehab M. Shaheen, "DS-UWB Pulse Design in IEEE802.15.3a Multipath Fading Channel for Cognitive Radio Applications," International Journal of Ultra Wideband Communications and Systems, 2016 Vol. 3 No. 3, pp. 155 – 165.

[28] Zhiquan Bai, et al., "Modified Chirp Waveforms-Based OCC-UWB System with Multiple Interferences Suppression," IEEE Systems Journal, Vol. 12, Issue 1, 2018.

[29] Maria-Gabriella Di Benedetto and Guerino Giancola, Understanding Ultra Wide Band Radio Fundamentals, Prentice Hall PTR, NJ, 2004.

[30] A. Giorgetti, and D. Dardari, "The Impact of OFDM Interference on TH-PPM/BPAM Transmission Systems," IEEE 61st Vehicular Technology Conference, Vol. 2, pp. 1037-1042, June 2005.

[31] Ehab M. Shaheen, and M. El-Tanany, "Narrowband Interference Impact on the Performance of UWB Communication Systems in Log-normal Flat Fading Channels," IEEE 71st Vehicular Technology Conference, VTC 2010-spring, 16-19 May 2010.

[32] L. Xiao, G. Xuan and Y. Wu, "Research on an improved chaotic spread spectrum sequence," 2018 IEEE 3rd International Conference on Cloud Computing and Big Data Analysis (ICCCBDA), Chengdu, 2018, pp. 420-423, doi: 10.1109/ICCCBDA.2018.8386553.